AMERICAN SOCIETY FOR MICROBIOLOGY | Journal of Virology®

VACCINES AND ANTIVIRAL AGENTS

Inhibition of Human Adenovirus Replication by the Importin $\alpha/\beta1$ Nuclear Import Inhibitor Ivermectin

Cason R. King,[a] Tanner M. Tessier,[a] Mackenzie J. Dodge,[a] Jason B. Weinberg,[b,c] Joe S. Mymryk[a,d,e]

[a]Department of Microbiology and Immunology, University of Western Ontario, London, Ontario, Canada
[b]Department of Pediatrics, University of Michigan, Ann Arbor, Michigan, USA
[c]Department of Microbiology and Immunology, University of Michigan, Ann Arbor, Michigan, USA
[d]Department of Oncology, University of Western Ontario, London, Ontario, Canada
[e]London Regional Cancer Program and Lawson Health Research Institute, London, Ontario, Canada

Cason R. King and Tanner M. Tessier contributed equally. Author order was determined based on seniority.

ABSTRACT Human adenoviruses (HAdV) are ubiquitous within the human population and comprise a significant burden of respiratory illnesses worldwide. Pediatric and immunocompromised individuals are at particular risk for developing severe disease; however, no approved antiviral therapies specific to HAdV exist. Ivermectin is an FDA-approved broad-spectrum antiparasitic drug that also exhibits antiviral properties against a diverse range of viruses. Its proposed function is inhibiting the classical protein nuclear import pathway mediated by importin-α (Imp-α) and -$\beta1$ (Imp-$\beta1$). Many viruses, including HAdV, rely on this host pathway for transport of viral proteins across the nuclear envelope. In this study, we show that ivermectin inhibits HAdV-C5 early gene transcription, early and late protein expression, genome replication, and production of infectious viral progeny. Similarly, ivermectin inhibits genome replication of HAdV-B3, a clinically important pathogen responsible for numerous recent outbreaks. Mechanistically, we show that ivermectin disrupts binding of the viral E1A protein to Imp-α without affecting the interaction between Imp-α and Imp-$\beta1$. Our results further extend ivermectin's broad antiviral activity and provide a mechanistic underpinning for its mode of action as an inhibitor of cellular Imp-$\alpha/\beta1$-mediated nuclear import.

IMPORTANCE Human adenoviruses (HAdVs) represent a ubiquitous and clinically important pathogen without an effective antiviral treatment. HAdV infections typically cause mild symptoms; however, individuals such as children, those with underlying conditions, and those with compromised immune systems can develop severe disseminated disease. Our results demonstrate that ivermectin, an FDA-approved antiparasitic agent, is effective at inhibiting replication of several HAdV types *in vitro*. This is in agreement with the growing body of literature suggesting ivermectin has broad antiviral activity. This study expands our mechanistic knowledge of ivermectin by showing that ivermectin targets the ability of importin-α (Imp-α) to recognize nuclear localization sequences, without effecting the Imp-$\alpha/\beta1$ interaction. These data also exemplify the applicability of targeting host factors upon which viruses rely as a viable antiviral strategy.

KEYWORDS E1A, adenoviruses, ivermectin, nuclear import

The continuous flow of molecules between the cytoplasm and nucleus of eukaryotic cells is essential for many cellular processes. Transport of macromolecules, especially proteins, across the nuclear envelope is a highly regulated process that requires passage through the nuclear pore complex (NPC) (1, 2). As protein size increases, so

Citation King CR, Tessier TM, Dodge MJ, Weinberg JB, Mymryk JS. 2020. Inhibition of human adenovirus replication by the importin α/β1 nuclear import inhibitor ivermectin. J Virol 94:e00710-20. https://doi.org/10.1128/JVI.00710-20.

Editor Lawrence Banks, International Centre for Genetic Engineering and Biotechnology

Address correspondence to Joe S. Mymryk, jmymryk@uwo.ca.

Received 15 April 2020
Accepted 2 July 2020
Accepted manuscript posted online 8 July 2020
Published 31 August 2020

does the difficulty in passing through the NPC. Larger proteins, typically over 40 to 50 kDa, require active transport mechanisms. This includes the classical protein nuclear import pathway which utilizes the importin alpha (Imp-α) and beta 1 (Imp-β1) proteins. Imp-α recognizes nuclear localization sequences (NLS) within proteins, while Imp-β1 serves to bridge the Imp-α/NLS complex with the NPC (3). Seven Imp-α isoforms exist in humans, all possessing a conserved importin beta binding (αIBB) domain located on their N terminus (4–6). The αIBB forms an intramolecular interaction with the NLS binding groove, preventing binding of Imp-β1 to an unloaded Imp-α, reducing futile nuclear translocation of empty import complexes (7). The Imp-α/β1 pathway defines classical nuclear import, where Imp-α recognizes NLSs containing a cluster of basic amino acids. These are collectively referred to as classical NLSs (3, 5, 8). By coevolving with eukaryotic hosts, viral pathogens have developed diverse mechanisms to usurp this important and highly coordinated pathway. These include mimicry of cellular NLSs by viral proteins and manipulation of these host factors at the molecular level (9).

Human adenoviruses (HAdVs) are ubiquitous in the human population, particularly in children and young adults, and contribute to a significant portion of respiratory and gastrointestinal illnesses worldwide (10–12). The most common HAdV species associated with disease are HAdV-C, -B, and -E (11). In particular, HAdV-B3 and -B7 are commonly associated with acute respiratory illness and have been reported in several outbreaks worldwide (13–17). HAdV-B55 has recently emerged as an epidemic strain in both Europe and Asia, causing acute respiratory illness in adults and outbreaks within civilian and military populations (18–21). Additionally, immunocompromised individuals, such as transplant recipients, are at particular risk for severe illness or death from numerous HAdVs, including HAdV-C, -A, and -B (11, 22). Aside from cidofovir, a nucleotide analogue approved for cytomegalovirus-induced retinitis, and the cidofovir derivative brincidofovir, there are no antiviral drugs with clinically relevant activity against HAdV (22, 23). Notably, HAdV gene expression, genome replication, and virion assembly all take place within the nucleus, and many of its gene products carry out crucial functions in this compartment to enhance its viral replication cycle (24, 25). This raises the possibility that drugs interfering with nucleocytoplasmic transport might inhibit HAdV replication. In addition to providing new molecular insights into the replication stages of HAdV infections, understanding the relationship between HAdV and host nuclear import machinery may identify target points for antiadenoviral therapies.

Ivermectin is a broad-spectrum antiparasitic approved for use in humans to treat a variety of neglected diseases, such as onchocerciasis and lymphatic filariasis, and has been mass administered for the treatment of scabies (26–30). Through a high-throughput drug-screening approach, ivermectin was also identified as a general inhibitor of Imp-α/β1-mediated nuclear import (31). Several recent studies have explored ivermectin as a means of abrogating nuclear localization of viral proteins and as an inhibitor of viral replication (9). Several RNA viruses, including human immunodeficiency virus (HIV), dengue virus (DENV), and Hendra virus (HeV), were potently inhibited *in vitro* by ivermectin (32–34). While findings on ivermectin's effects on DNA viruses are more limited, it has been shown to impair BK polyomavirus (BKPyV) infection *in vitro* (35).

In this study, we sought to extend the exploration of ivermectin's antiviral activity by examining its effects on HAdV-C5 infection. We found that ivermectin inhibits the overall production of infectious HAdV-C5 progeny in a dose-dependent fashion. Multiple viral proteins produced early during infection exhibited impaired nuclear localization. Ivermectin treatment led to severely reduced levels of several HAdV-C5 mRNAs, protein products, and progeny genomes postinfection. In addition, we show that ivermectin targets the Imp-α/NLS interaction without disrupting Imp-β1 binding. Together, these findings offer insight into ivermectin's inhibitory effects on HAdV replication, as well as provide new mechanistic details regarding ivermectin's mode of action.

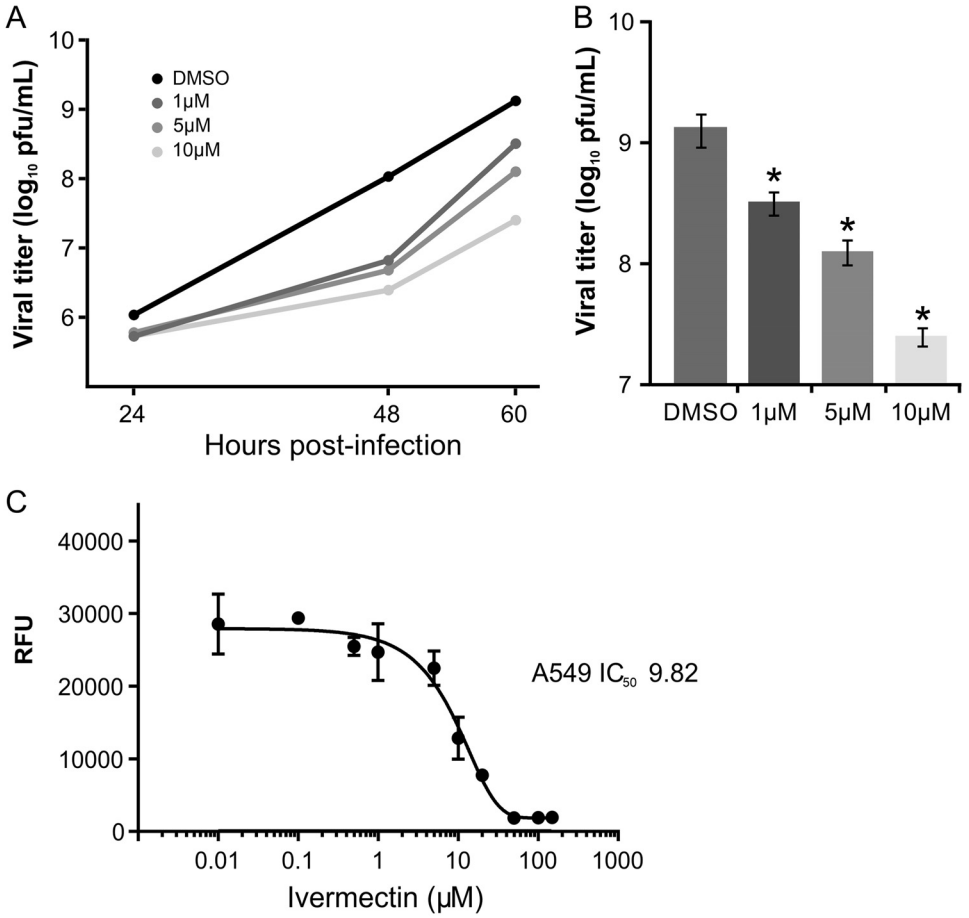

FIG 1 Ivermectin inhibits production of infectious HAdV progeny in a dose-dependent manner. A549 cells were infected with HAdV-C5 (MOI 5) and treated with up to 10 μM ivermectin. Cells were collected at various time points up to 60 hours postinfection, when cytopathic effect had cleared most cells. Production of infectious progeny virus quantitatively assayed by plaque formation on HEK293 cells. (A) Data are shown over 24 to 60 hours for a range of ivermectin doses. (B) Data at the 60-hour endpoint are highlighted, and statistical significance is shown relative to DMSO control-treated cells. Values are represented as mean ± SEM. *, $P < 0.01$; $n = 3$. (C) A549 cells were subjected to a 72-hour dose of ivermectin at various concentrations to gauge long-term cell viability using a PrestoBlue assay.

RESULTS

Ivermectin inhibits HAdV-C5 progeny production in a dose-dependent manner. Ivermectin has been previously demonstrated to function as an antiviral agent against several viruses that encode factors that rely on host Imp-α/β1-mediated nuclear transport (31). Ivermectin has been described as a general inhibitor of this pathway and was shown to reduce nuclear import of viral proteins such as SV40 large T-antigen (TAg), HIV integrase, DENV NS5, and BKPyV VP2 and VP3 (32–35). To build upon these initial studies, we sought to test this drug's ability to affect HAdV replication, as it too encodes many proteins with crucial nuclear functions (36).

A549 lung epithelial carcinoma cells were infected with HAdV-C5 at a multiplicity of infection (MOI) of 5 over a range of ivermectin concentrations and harvested at various time points postinfection to determine viral titers (Fig. 1A). Compared to DMSO (dimethyl sulfoxide) control-treated cells, production of infectious progeny from cells treated with ivermectin was significantly reduced. Observed differences emerged as early as 24 hours postinfection (hpi), continuing through to 60 hpi (Fig. 1B). Notably, higher doses of ivermectin corresponded with more potent inhibition of progeny production, indicative of a dose-dependent response. The doses ranged from concentrations that did not affect cell health (1 μM), up to its 50% inhibitory concentration

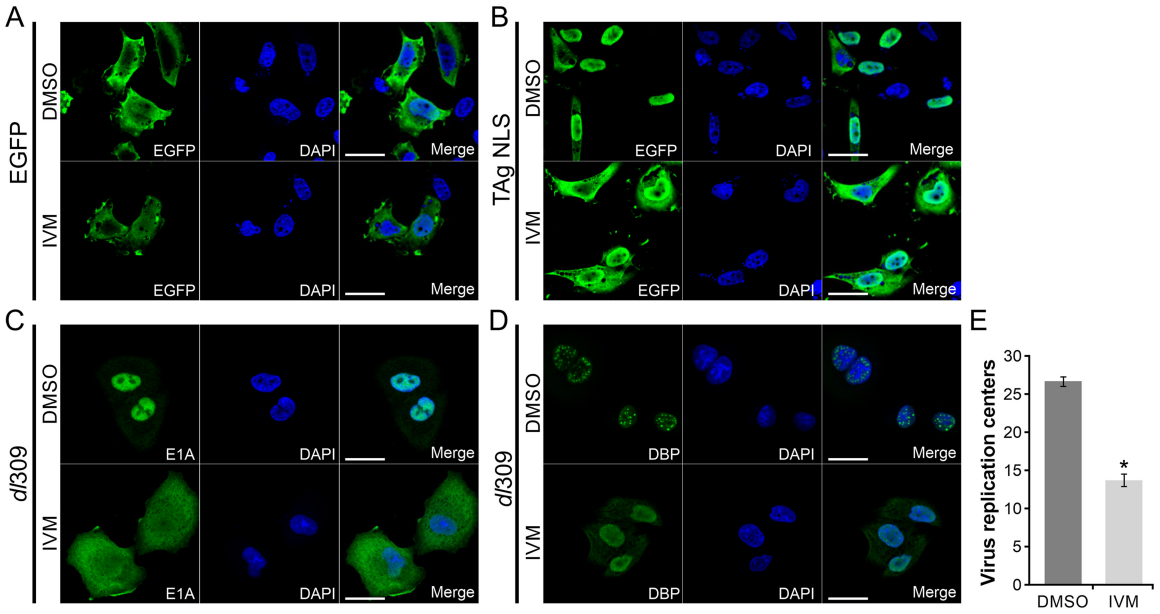

FIG 2 Ivermectin blocks Imp-α-mediated nuclear localization of proteins crucial for HAdV infection. (A and B) HT-1080 cells were transfected with either EGFP (vector) or EGFP-tagged T-antigen NLS and treated with 25 μM ivermectin (IVM) for 1.5 hours prior to fixation and immunofluorescence imaging. Cytoplasmic relocalization of T-antigen NLS in the presence of ivermectin serves as a positive control for IVM's function. (C and D) A549 cells were infected with HAdV-C5 (MOI, 5) and treated with 10 μM IVM for 20 hours until cells were fixed and processed for imaging. (C) Subcellular localization of E1A during infection in the presence of ivermectin. (D) DBP immunofluorescence as a surrogate for viral replication centers reveals smaller and fewer virus replication centers. (E) Quantification of the viral replication centers in panel C as determined by DBP immunofluorescence (displayed as means $\pm$ SEM; *, $P < 0.001$; $n = 50$). Scale bars represent 25 μm.

(IC_{50}) as indicated by cell viability assays performed 72 hours postadministration (Fig. 1C). For experiments where longer exposures (12 to 60 hours) of ivermectin were required, we chose 10 μM as our working concentration, whereas short-term experiments (<6 hours) used higher doses, consistent with the existing literature (37).

Ivermectin abrogates nuclear localization of viral factors crucial for the HAdV-C5 replication cycle. To determine how ivermectin was inhibiting HAdV-C5 replication, we examined its impact on the subcellular localization of several HAdV-C5 proteins with known nuclear functions. As proof of principle, we first sought to reproduce previously published findings demonstrating ivermectin's ability to block nuclear import of an enhanced green fluorescent protein (EGFP)-tagged T antigen (TAg) NLS. The SV40 TAg NLS is one of the oldest and most well-characterized classical NLSs and relies exclusively on Imp-α/β1 for import (38). HT-1080 fibrosarcoma cells were transfected with either EGFP or EGFP-TAg NLS and subsequently treated for 1.5 hours with 25 μM ivermectin or DMSO control. As anticipated, EGFP localization was unaffected by treatment with ivermectin (Fig. 2A). While EGFP-TAg NLS protein was predominantly nuclear in control-treated cells, there was a noticeable shift to cytoplasmic accumulation in ivermectin-treated cells (Fig. 2B). Importantly, 25 μM ivermectin for 1.5 hours did not elicit any observable cytopathic effects with the HT-1080 cell line. This result confirms that ivermectin reduces nuclear import mediated by the classical SV40 TAg NLS in this experimental system.

Next, we examined ivermectin's effects on several HAdV-C5 early gene products during infection of A549 cells. We specifically targeted E1A and DNA-binding protein (DBP), two proteins which utilize the Imp-α/β1 machinery. HAdV E1A is a multifunctional protein and is the first HAdV gene product synthesized postinfection (39). It functions by binding and altering the functionality of dozens of cellular target proteins to drive viral transcription and induce the S phase of the cell cycle (39). E1A contains a classical NLS that utilizes Imp-α/β1 to facilitate its nuclear import and exhibits a predominantly nuclear localization (40–42). Compared to control-treated cells, 10 μM

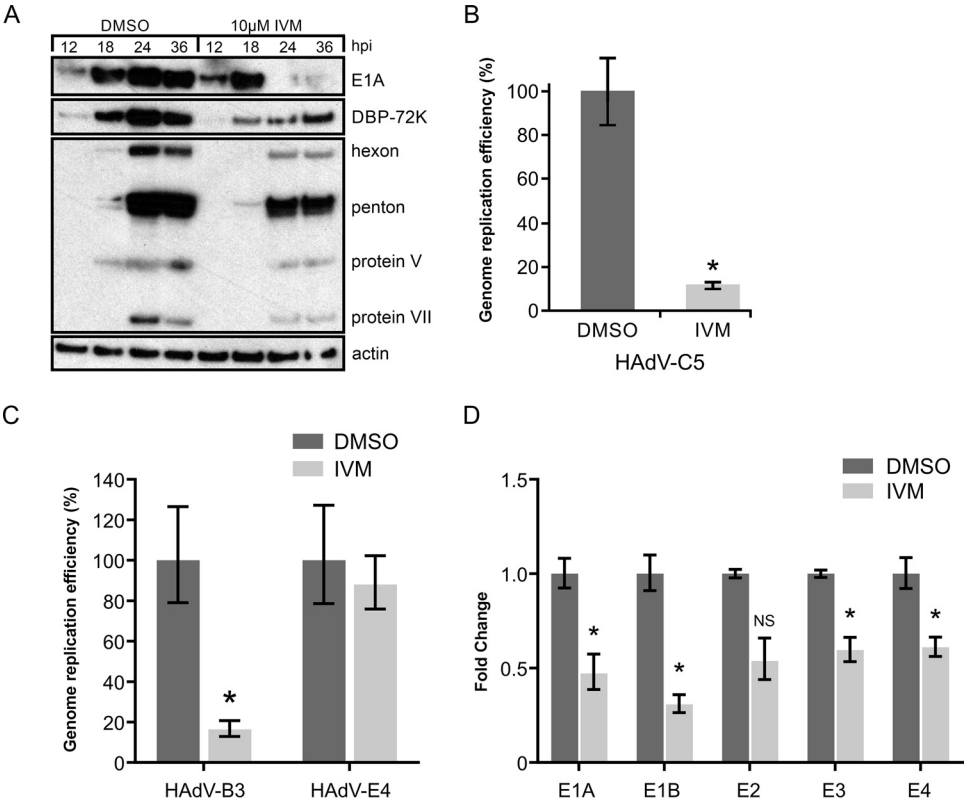

FIG 3 Ivermectin impairs the molecular kinetics of HAdV infection on multiple levels. A549 cells were infected (MOI, 5) with HAdV-C5 (A, B, D), HAdV-B3, or -E4 (C) and treated with 10 μM ivermectin (IVM). (A) Cells were harvested at 12, 18, 24, and 36 hpi, and viral protein synthesis was assayed by Western blotting using antibodies against representative proteins from various HAdV-C5 transcription units. Actin was used as a loading control. (B and C) DNA was isolated at 6 hpi as a measure of viral input and at 48 hpi. Relative viral genomic DNA levels were quantified by qPCR using a forward primer recognizing a conserved sequence in the left end of the HAdV genome in combination with specific reverse primers for HAdV-C5, -B3, and -E4. To determine viral genome replication efficiency, 48 hpi was normalized to the 6 hpi input. IVM treatment significantly impaired efficiency of HAdV-C5 and -B3 genome replication, represented as mean ± SEM (*, $P < 0.005$; $n = 3$). (D) RNA was isolated at 24 hpi, and cDNA was generated using random primers. RT-qPCR was performed targeting HAdV-C5 early gene products, and results were normalized to cellular GAPDH. Fold change compared to control-treated cells is shown, displayed as mean ± SEM; *, $P < 0.05$; NS, not significant; $n = 3$.

ivermectin caused a dramatic increase in cytoplasmic localization of E1A at 20 hpi (Fig. 2C). HAdV DBP is a single-stranded DNA-binding protein encoded by the viral E2A early gene and coats single-stranded DNA intermediates of HAdV genome replication (43). In addition, visualization of DBP in HAdV-infected cells serves as a surrogate marker for virus replication centers (44). Like E1A, DBP also contains a classical NLS (45). While treatment of cells with 10 μM ivermectin did not elicit a drastic shift of DBP to the cytoplasm like it did with E1A (Fig. 2D), noticeably smaller and fewer virus replication centers were present in the nuclei of infected cells at 20 hpi (Fig. 2E).

Ivermectin impairs viral transcription, genome replication, and protein synthesis. To further gauge ivermectin's effects on the molecular kinetics of HAdV-C5 infection, we analyzed multiple aspects of the HAdV-C5 replication cycle. The decreased levels of infectious progeny produced after ivermectin treatment (Fig. 1) could be due to reduced expression of crucial viral proteins. We first examined overall levels of both early (E1A and DBP) and late (hexon, penton, and protein V and VII) HAdV-C5 proteins across multiple infection time points (Fig. 3A). We observed numerous defects in HAdV-C5 protein production in the presence of 10 μM ivermectin. While the initial burst (12 to 18 hpi) of E1A synthesis appeared unaffected, subsequent time points (24 to 36 hours) displayed a large reduction in E1A protein levels as shown by Western blotting. Similarly, DBP and all late proteins were expressed at lower levels in cells treated with ivermectin across all time points.

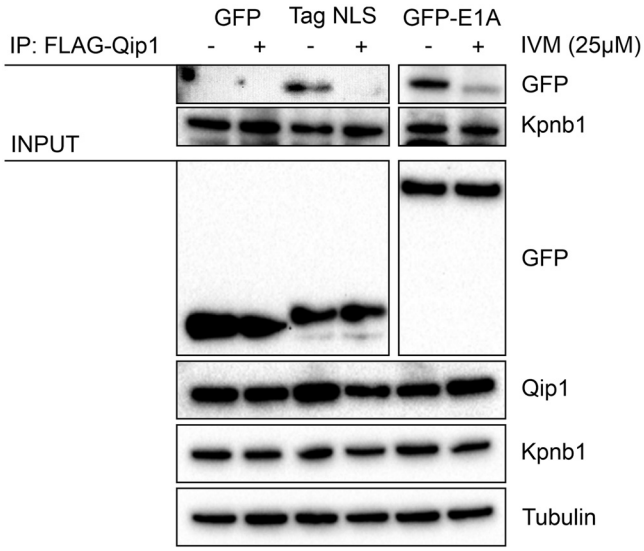

FIG 4 Ivermectin blocks NLS binding, but not the Imp-α and -β1 interaction. HT-1080 cells were cotransfected with either EGFP-tagged TAg NLS or HAdV-C5 E1A as well as FLAG-tagged Qip1 (importin-α3). Prior to coimmunoprecipitation, cells were pretreated with 25 μM ivermectin (IVM) or DMSO and then immunoprecipitated (FLAG) in the presence of 25 μM IVM or DMSO. Western blots for both EGFP constructs and endogenous Kpnb1 (Imp-β1) were performed on the same FLAG-Qip1 immunoprecipitated samples. In the presence of ivermectin, Qip1 is unable to recognize both TAg NLS and E1A protein. Under these conditions, the interaction between Qip1 and Imp-β1 was unaffected by IVM.

We next tested if ivermectin was affecting replication of the viral DNA genome itself. As a consequence of the reduced levels of DBP and lower numbers of virus replication centers (Fig. 2D), we suspected that viral genome copy numbers would be reduced. Indeed, compared to DMSO-treated cells, ivermectin treatment caused a significant decrease in viral genome replication efficiency at 48 hpi as measured by quantitative PCR (qPCR) for HAdV-C5 (Fig. 3B). To determine if ivermectin is effective against other clinically relevant HAdV species, we tested genome replication efficiency for both HAdV-B3 and HAdV-E4 (Fig. 3C). Similar to HAdV-C5, a significant reduction in HAdV-B3 genome replication was observed. However, HAdV-E4 was unaffected by ivermectin under these conditions.

E1A is a necessary transcriptional activator (*trans*-activator) of HAdV-C5 early gene expression (39). We hypothesized that ivermectin-mediated abrogation of its nuclear localization and overall expression (Fig. 2C and 3A) would cause reduction of E1A-regulated viral transcripts. We examined HAdV-C5 infected cells at 24 hpi (when E1A protein levels showed a large difference between DMSO and ivermectin treatment [Fig. 3A]) for expression of the E1A, E1B, E2, E3, and E4 transcription units using reverse transcriptase quantitative PCR (RT-qPCR) (Fig. 3C). All early genes displayed reduced levels of mRNA expression in the presence of ivermectin, consistent with our hypothesis.

Ivermectin inhibits the Imp-α/NLS interaction, but not the Imp-α/β1 interaction. Although ivermectin directly targets the classical nuclear import pathway, the exact molecular mechanism by which it inhibits nuclear import remains unclear. Ivermectin's mode of action could be via blocking NLS recognition by Imp-α, blocking the Imp-α/β1 interaction, or possibly both. To provide mechanistic insight into ivermectin's impact on nuclear import, we tested its effects on the protein-protein interaction between classical NLSs and Imp-α. We cotransfected HT-1080 cells with FLAG-tagged Qip1 (Imp-α3) and either EGFP-tagged TAg NLS or HAdV-C5 E1A and subjected whole-cell lysates to coimmunoprecipitation (CoIP) in the presence of ivermectin (Fig. 4). Immunoprecipitation of Qip1 showed significantly reduced binding to either the TAg NLS or E1A in the presence of ivermectin compared to the DMSO control. Since nuclear import of cargo by Imp-α depends on Imp-β1, we also tested for Qip1's ability

to pull down endogenous Imp-β1 (Kpnb1) using the same CoIP samples. In contrast to cargo interactions, the concentration of ivermectin sufficient to inhibit TAg NLS or E1A binding was not sufficient to block binding of endogenous Imp-β1 to Qip1. These results suggest that ivermectin specifically inhibits the ability of Imp-α to recognize a classical NLS, without affecting the Imp-α/β1 interaction.

DISCUSSION

Cellular pathways controlling nuclear-cytoplasmic transport of viral proteins have emerged as attractive targets for antiviral intervention. The search for new targets is partly due to existing limitations of directly acting antivirals, which often utilize a "one drug, one bug" approach (46). Most of the approved antivirals target virally encoded enzymes (47), which inherently have a narrow spectrum of activity when considering the vastness of viral diversity. Emerging viruses such as severe acute respiratory syndrome coronavirus (SARS-CoV), Middle East respiratory syndrome CoV (MERS-CoV), and SARS-CoV-2 have no directly acting antiviral treatments, highlighting an area where broadly acting antivirals could have profound impact (48, 49).

One approach to developing broadly acting antivirals is through targeting host factors upon which the virus depends. Evolution of resistance to a drug is expected to be much slower, or even nonexistent, for a host factor than for a virus. Targeting these weak points of virus-host interfaces is a strategy being aggressively explored for numerous viruses (50–52). Success has even been achieved with antiretroviral compounds that target the host coreceptor CCR5, blocking HIV replication (53).

Intracellular pathways, such as protein nuclear import, are exploited by many RNA and DNA viruses. Many viruses replicate their genomes within the nucleus of infected cells and/or encode *trans*-acting viral proteins with important nuclear functions. Also, many protein components of nuclear transport pathways are directly hijacked by diverse viruses (9, 39). Among these is the classical nuclear import pathway mediated by Imp-α/β1, making it an actionable host target for broadly acting antivirals. Several drugs, including small molecules and peptides, have been shown to target this pathway (54). However, only two of these, ivermectin and mifepristone, are FDA approved, albeit for nonviral indications (54–56). A novel high-throughput screening approach identified ivermectin as a specific inhibitor of nuclear import of HIV integrase via inhibition of this pathway (31). To date, ivermectin has been shown to inhibit nuclear import of viral proteins from a range of viruses *in vitro* (32, 33, 55, 57–61) and is currently being used in a clinical trial for the treatment of pediatric dengue virus patients (NCT03432442). Further highlighting the potential application of ivermectin is recent evidence demonstrating that ivermectin can inhibit replication of SARS-CoV-2 *in vitro* (62). Together, these findings map a new direction for studying these classes of drugs, particularly ivermectin, as potentially useful broad-spectrum antiviral agents.

Here, we sought to examine ivermectin's effects on HAdV infection, using HAdV-C5 as a model. Treatment of cells with ivermectin after infection with HAdV-C5 resulted in a dose-dependent decrease in the production of infectious progeny virus as determined by plaque assay. This reduction was most severe in the presence of 10 μM ivermectin, which caused a nearly 2-fold log reduction in viral titers at 60 hpi compared to DMSO-treated control cells. While this dose of ivermectin did begin to negatively affect cell health at 72 hours postadministration, this is unlikely to account for the nearly 100-fold reduction in viral output, especially as experimental samples were collected earlier than 72 hours. These results parallel recent findings demonstrating that ivermectin can inhibit production of infectious progeny from other viruses, including flaviviruses such as West Nile virus, Zika virus, and DENV (61).

To begin to understand how ivermectin inhibits HAdV-C5 replication, we explored the impact of ivermectin on intracellular localization of HAdV proteins during infection. We first confirmed ivermectin's ability to block Imp-α-mediated nuclear import by using the well-characterized classical SV40 TAg NLS as a control. Like TAg, the HAdV-C5 E1A protein also contains a classical NLS that utilizes Imp-α/β1 to drive nuclear import (40). After infection with HAdV-C5, treatment with 10 μM ivermectin caused a shift in E1A

subcellular localization from its predominantly nuclear localization to a nuclear/cytoplasmic one, similar to that observed for a mutant E1A containing a deletion of its C-terminal NLS sequence (63). While most E1A was relocalized to the cytoplasm, some remained in the nucleus. This may be due to insufficient drug, or E1A's small size, which may allow some passive diffusion into the nucleus. Additionally, E1A has several nonclassical NLSs, which may allow entry into the nucleus in the absence of the classical nuclear import (64). Nevertheless, use of such alternative nuclear import pathways is clearly not sufficient for the virus to overcome the negative effects caused by ivermectin's inhibition of classical nuclear import.

We also examined the localization of HAdV-C5 DBP, a single-stranded DNA-binding protein. DBP is a larger (~72 kDa) protein crucial for replication of the viral genome and is frequently used as a marker for visualizing virus replication centers (43). Interestingly, ivermectin did not affect DBP nuclear localization as dramatically as E1A, despite the known presence of two classical NLSs within its N terminus. This was not entirely unexpected, as a previous study showed that mutant DBP lacking its NLSs was still strongly nuclear (45). Since ivermectin only targets Imp-α cargo, it remains possible that DBP utilizes an Imp-α-independent nuclear import pathway. Nevertheless, ivermectin treatment affected the formation of virus replication centers, as they were smaller and fewer, in concordance with the observed lower levels of viral progeny production.

In addition to infectious progeny, we surveyed the impact of ivermectin treatment on HAdV-C5 early and late proteins, as well as replication of its DNA genome. On the protein level, synthesis of E1A at early time points during infection remained unchanged. This may be due to E1A's initial expression being driven by a strong, constitutive enhancer sequence in the left end of the HAdV genome (65). It also suggests that the earliest parts of HAdV-C5 infection may be unaffected by disruption of the Imp-α/β1 pathway. This is different from the effect of ivermectin on infection by BKPyV, another small DNA tumor virus. BKPyV utilizes classical NLSs to facilitate nuclear entry of incoming viral particles (35), while HAdV capsids transit to the nucleus via microtubules in an NLS-independent manner (66, 67). Despite the initial burst of E1A expression in the presence of ivermectin, subsequent time points showed a severe loss of E1A protein synthesis after 24 h. This suggests that the positive feedback loop whereby newly synthesized E1A protein would enter the nucleus to transactivate additional expression of itself may be disrupted by ivermectin. Levels of DBP were decreased across infection, consistent with the smaller amounts of virus replication centers previously observed. Expression of various late proteins, including hexon, penton, and protein V and VII, were also greatly reduced in the presence of ivermectin. As expected, overall replication of the HAdV-C5 genome was severely decreased by ivermectin treatment. This aligns with observations of the smaller numbers of virus replication centers and overall lower expression levels of DBP. The combination of reduced viral genome templates and early proteins also likely accounts for the subsequent reduction in HAdV-C5 late gene expression.

In addition to HAdV-C5, we tested genome replication efficiency for HAdV-B3 and -E4, both of which represent clinically relevant HAdV species. Like HAdV-C5, ivermectin dramatically reduced HAdV-B3 genome replication. HAdV-B3 is commonly associated with acute respiratory illness; therefore, drugs like ivermectin could have significant clinical relevance. For HAdV-E4, overall levels of replication were lower than for -B3 and -C5 even in DMSO-treated cells, but its relative genome replication was unaffected by ivermectin treatment. Although initially surprising, the lower replicative ability of this virus could obscure ivermectin's effects. Alternatively, HAdV-E4 is unique among HAdVs, as it more closely resembles simian adenoviruses (68). Past studies examining HAdV-E4 genome replication suggest that HAdV-E4 relies on a different repertoire of host factors than other HAdV species (63). For example, knockdown of host protein kinase A severely inhibits genome replication of HAdV-B3, -C5, -D9, and -A12, but not -E4. Furthermore, *in vitro* evidence has demonstrated that the E1A protein of HAdV-E4 uses a nonclassical NLS located in conserved region 3. Indeed, E1A from HAdV-B3 and -C5 also possesses this nonclassical NLS; however, nuclear import studies have shown

this region of HAdV-E4 E1A to be a much more potent stimulator of nuclear import than -B3 or -C5 (64).

Lastly, we probed for relative expression levels of mRNAs from all HAdV-C5 early transcription units (E1A, E1B, E2, E3, and E4). At 24 hpi, we detected lower levels of mRNA for each of these early genes. This is expected given the lower levels of E1A expression, which would otherwise drive higher expression of these downstream genes (39). Together, these findings suggest ivermectin's inhibition of HAdV-C5 replication stems mostly from lower expression of crucial viral gene products, particularly E1A, via disruption of its nuclear localization.

Despite the growing interest in studying ivermectin as an antiviral agent, relatively little is known about its molecular mode of action. The original high-throughput drug screen unequivocally demonstrated ivermectin's ability to inhibit the binding of HIV integrase and TAg NLS to the Imp-α/β1 complex. Recent *in vitro* data published by Yang et al., suggest that ivermectin induces structural changes in Imp-α that prevents NLS recognition, as well as binding to Imp-β1 (61). Our data derived from CoIP experiments confirm that ivermectin blocks NLS recognition. However, our results suggest that concentrations of ivermectin sufficient to block NLS binding to Imp-α are not sufficient to disrupt formation of the Imp-α/β1 complex. The αIBB domain of Imp-α acts as an auto-inhibitory NLS that binds its own NLS binding region in a fashion that mimics classical NLS binding (69). Ivermectin could theoretically block or weaken this intramolecular interaction the same way it blocks NLS binding, while leaving the αIBB/Imp-β1 intermolecular interaction unaffected. It would be interesting to determine if Imp-β1 is still carrying unloaded Imp-α into the nucleus in the presence of ivermectin, causing futile cycles of import that may have consequences beyond simple inhibition of NLS/Imp-α interactions. Although we examined Qip1 (Imp-α3) in detail, as it is the preferred importin for E1A (42), it will be important to consider how ivermectin may influence NLS binding to other Imp-α isoforms. Differences among isoforms can influence both the binding of NLSs and the auto-inhibitory potential of the αIBB (6). This could be achieved by studying the broader effects of ivermectin with a panel of different Imp-α isoforms and a variety of classical NLSs.

Based on the data presented here, we conclude that the effect of ivermectin on nuclear import of E1A can explain the significant reduction in viral replication (Fig. 5). Upon HAdV infection, E1A is the first viral gene transcribed and is responsible for setting the stage for viral replication to proceed (70, 71). Inhibition of E1A nuclear import at early time points during infection would impair its ability to transactivate viral early genes, including itself, ultimately resulting in the downstream consequences observed here: impaired production of other early proteins, genome replication, late proteins, and infectious progeny. Supporting this, orthogonal experiments using HAdV encoding an NLS-deleted E1A showed a similar reduction in overall viral replication as we see here with ivermectin (72).

In summary, this study provides evidence that disruption of classical Imp-α/β1-mediated nuclear import has promise in combating at least a subset of HAdV infections. Importantly, these data support the growing body of literature suggesting ivermectin has utility as a broadly acting antiviral agent. In addition, these findings demonstrate the strategic advantage of targeting host factors for antimicrobial action. Genetically distinct viruses often share important, potentially druggable features as a result of their codependence on host processes, including the classical nuclear import pathway (9, 35, 73, 74). In addition to repurposing ivermectin for treatment of viral infections that have no current therapeutic options (including HAdV), these results support the idea that targeting host nuclear import by other drugs or means could be a valid strategy as well.

MATERIALS AND METHODS

Cell lines, cell culture, and transfections. Human A549 (provided by Russ Wheeler, Molecular Pathology/Genetics, London Health Sciences Centre), HEK293, and HT-1080 (purchased from the American Type Culture Collection) cells were grown at 37°C with 5% CO_2 in Dulbecco's modified Eagle's medium (DMEM; Multicell Technologies) supplemented with 1% penicillin/streptomycin (Multicell) and 10% fetal bovine serum (FBS; Gibco). Transfection of DNA into HT-1080 cells was done using

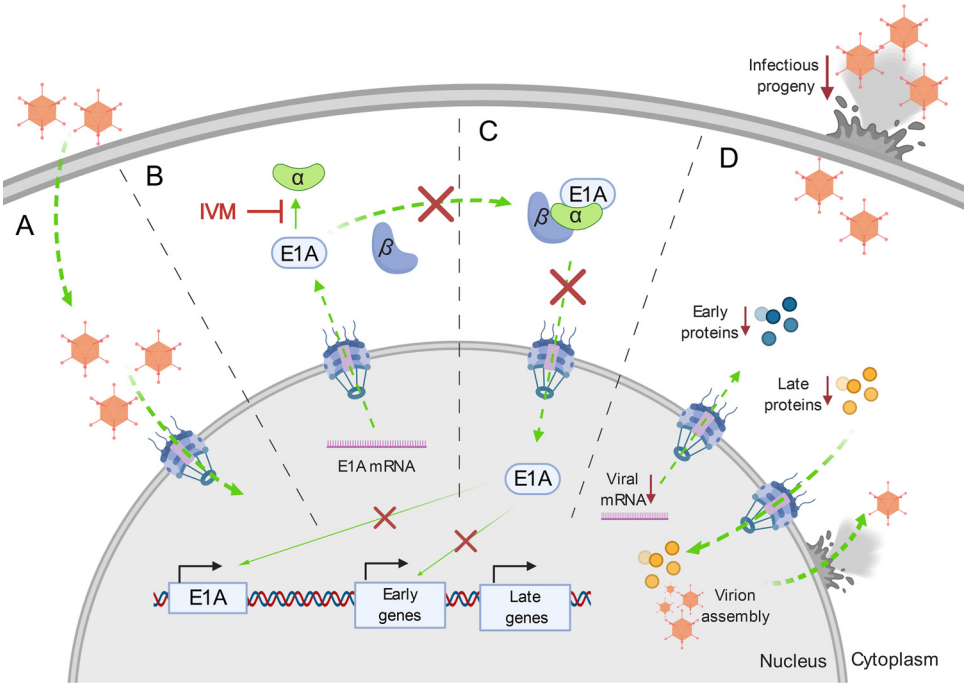

FIG 5 Ivermectin-mediated inhibition of the HAdV replication cycle. Proposed model of how ivermectin (IVM) inhibits adenovirus replication. Green arrows indicate normal viral processes. Those processes inhibited directly or indirectly by IVM are labeled with red. (A) HAdV virions are trafficked to the nuclear pore complex (NPC) via microtubules, and viral genomes are released into the nucleus. (B) E1A is transcribed immediately, and its corresponding mRNA is translated within the cytoplasm. In the presence of IVM, E1A protein cannot bind importin alpha (α, green), therefore preventing the formation of a competent E1A/importin-α/β1 import complex. (C) In the presence of IVM E1A, protein is not efficiently imported into the nucleus, indirectly preventing further transcription of E1A and induction of other viral early genes. (D) Reduced expression of viral gene products leads to reduced genome replication, late proteins, and ultimately, the assembly of viral progeny within the nucleus.

X-tremeGENE HP (Roche) by following the manufacturer's recommendations. For treatment with ivermectin on transfected HT-1080 cells, medium was replaced 16 hours posttransfection with fresh DMEM containing 10% FBS and the indicated concentration of drug (or the corresponding volume of DMSO control) and left for 1.5 hours prior to downstream harvesting for microscopy or immunoprecipitation.

Viruses and infection of cells. Wild-type (WT) HAdV-C5 (*dl*309) was previously described (75). WT serotypes of HAdV-3 (strain GB, lot 11W) and -4 (strain RI-67, lot 3W) were purchased from the ATCC via Cedarlane. A549 cells were infected at an MOI of 5 PFU/ml. Cell cultures were infected at ~50% confluence for 1 hour at 37°C, and subconfluent cells were collected at the indicated time points for downstream experiments. For plaque assays, confluent HEK293 cells were infected with serially diluted samples for 1 hour at 37°C before being overlaid with DMEM containing 1% SeaPlaque agarose (Lonza). For treatment with ivermectin on infected A549 cells, infectious medium was replaced after 1 hour with fresh DMEM containing 10% FBS and the indicated working concentrations of drug (or the corresponding volume of DMSO control) for the duration of the experiment.

Cell viability assay. Cells were seeded in 96-well plates at 2,500 cells per well and left to adhere overnight. Medium containing ivermectin was added at concentrations ranging from 10 nM to 150 μM and left for 72 hours before viability was assessed. For each condition, three replicates were used. Viability was indirectly measured using PrestoBlue reagent (Thermo Fisher). Normalized relative fluorescent units (RFUs) of the ivermectin-treated replicates were calculated as a percentage of the mean RFU of control (DMSO-only) treatment replicates. IC_{50} values, defined as the concentration at which the normalized RFU reached 50%, were calculated by nonlinear regression (Prism 8; GraphPad Software, Inc.).

Plasmids. All constructs were expressed in vectors under the control of the cytomegalovirus (CMV) promoter. Full-length E1A and TAg NLS constructs were built into pEGFP-C2. FLAG-tagged Qip1 was cloned into pcDNA3 and contains a full-length WT importin-α3 (KPNA4) and was previously described (64).

Coimmunoprecipitation and Western blotting. Cells were pretreated with 25 μM ivermectin for 1.5 hours prior to lysis. Cells were lysed in 500 μl NP-40 lysis buffer (150 mM NaCl, 50 mM Tris-HCl pH 7.5, 0.1% NP-40) supplemented with protease inhibitor cocktail (MilliporeSigma; P8340). Coimmunoprecipitation reactions were carried out at 4°C for 4 hours in NP-40 buffer supplemented with either 25 μM ivermectin or an equivalent volume of DMSO, using 20 μl of washed magnetic FLAG beads (MilliporeSigma; M8823). Two percent of the sample was kept as input control. After being washed with NP-40 buffer, complexes were boiled in 25 μl of lithium dodecyl sulfate (LDS) sample buffer for 5 minutes. Samples were separated on NuPage Bis-Tris gels (Life Technologies) and transferred onto a polyvi-

nylidene difluoride membrane (Amersham). Membranes were blocked in 5% skim milk constituted in Tris-buffered saline (TBS) with 0.1% Tween 20. Primary antibodies used include rabbit α-EGFP (Clontech), mouse α-E1A (clone M73; in-house), mouse α-DBP (clone B6-8; in-house), mouse α-karyopherin β1 (Santa Cruz; sc-137016), and rabbit α-HAdV5 (Abcam). Horseradish peroxidase-conjugated secondary antibody was detected using Luminata Crescendo or Forte substrate (Millipore).

Immunofluorescence microscopy. Cells were fixed in 3.7% paraformaldehyde at room temperature, permeabilized on ice using 0.2% Triton X-100, and blocked using 3% BSA in phosphate-buffered saline (PBS). Samples were incubated in primary antibody (rabbit α-EGFP [Clontech], mouse α-E1A [clone M73; in-house], mouse α-DBP [clone B6-8; in-house]) for 1 hour at room temperature and another 30 minutes at room temperature with secondary antibody (Alexa Fluor 488; Life Technologies). Samples were mounted with Prolong Gold reagent containing 4′,6-diamidino-2-phenylindole (DAPI; Life Technologies). Confocal images were acquired using a Fluoview 1000 laser scanning confocal microscope (Olympus Corp.).

Reverse transcription and qPCR. Total RNA was prepared using the PureLink RNA minikit (Thermo Fisher) including on-column PureLink DNase treatment. RNA was reverse-transcribed into cDNA using the Superscript VILO Mastermix (Thermo Fisher). Relative cDNA levels were measured by qPCR using Power SYBR green (Thermo Fisher) with oligonucleotide sequences that specifically recognize the indicated HAdV-C5 targets (E1A [forward (F), ACACCTCCTGAGATACACCC; reverse (R), TTATTGC CCAGGCTCGTTAAGC], E1B [F, GACAATTACAGAGGATGGGC; R, CACTCAGGACGGTGTCTGG], E2 [F, GGGGGTGGTTTCGCGCTGCTCC; R, GCGGATGAGGCGGCGTATCGAG], E3 [F, GAGGCAGAGCAACTGC GCC; R, GCTCTCCCTGGGCGGTAAGCCGG], E4 [F, GCCCCCATAGGAGGTATAAC; R, GGCTGCCGCTGTGG AAGCGC]). GAPDH (F, ACTGCTTAGCACCCCTGGCCAA; R, ATGGCATGGACTGTGGTCATGAGTC) was used as an endogenous cellular control for total cDNA along with no-RT and no-template negative controls. Results were normalized to cellular GAPDH, calculated using the $\Delta\Delta CT$ method, and set as relative to DMSO-treated samples.

Virus replication assay. A549 cells were infected with either HAdV-C5, -B3, or -E4 and then supplemented with medium containing 10 μm ivermectin. Total cell DNA was purified at 6 and 48 hours postinfection using a DNeasy blood and tissue kit (Qiagen). Viral DNA levels were quantified by qPCR with Power SYBR green (Thermo Fisher) using a forward (F) primer (E1A-F, AGAGGCCACTCTTGAGTGC) that recognizes a conserved sequence in E1A in combination with a HAdV-C5-specific reverse (R) primer (Ad5E1A-R, CGTCACGTCTAAATCATAC), HAdV-B3-specific reverse (R) (Ad3E1A-R, TACAGATCGTGCAGCGT AGG), or HAdV-E4-specific reverse (R) primer (Ad4E1A-R, AGCGAAGGTGTCTCAAATGG). Values were normalized to GAPDH (F, ACTGCTTAGCACCCCTGGCCAA; R, ATGGCATGGACTGTGGTCATGAGTC), and the fold increase of viral copy number at 48 hours was calculated by normalizing to input viral DNA at 6 hours postinfection. Viral replication efficiency in the presence of ivermectin was presented as the relative value compared to that for DMSO control-treated cells, which were normalized to 1.

Statistical analysis. All experiments were carried out with three biological replicates. Graphs represent means and standard errors of the means (SEM) for all biological replicates. For Western blotting, a representative image was selected. Statistical significance of numerical differences was calculated using either *t* tests or one-way analysis of variance and Holm-Sidak *post hoc* comparisons between experimental conditions.

ACKNOWLEDGMENTS

This work was supported by grants from the Canadian Institute of Health Research (MOP-148689) to J.S.M. and the National Institutes of Health (R21 AI142073) to J.B.W. C.R.K. and T.M.T. were supported by Ontario graduate scholarships.

REFERENCES

1. Bauer NC, Doetsch PW, Corbett AH. 2015. Mechanisms regulating protein localization. Traffic 16:1039–1061. https://doi.org/10.1111/tra.12310.
2. Cautain B, Hill R, de Pedro N, Link W. 2015. Components and regulation of nuclear transport processes. FEBS J 282:445–462. https://doi.org/10.1111/febs.13163.
3. Lange A, Mills RE, Lange CJ, Stewart M, Devine SE, Corbett AH. 2007. Classical nuclear localization signals: definition, function, and interaction with importin. J Biol Chem 282:5101–5105. https://doi.org/10.1074/jbc.R600026200.
4. Cingolani G, Petosa C, Weis K, Müller CW. 1999. Structure of importin-β bound to the IBB domain of importin-α. Nature 399:221–229. https://doi.org/10.1038/20367.
5. Kelley JB, Talley AM, Spencer A, Gioeli D, Paschal BM. 2010. Karyopherin α7 (KPNA7), a divergent member of the importin α family of nuclear import receptors. BMC Cell Biol 11:63. https://doi.org/10.1186/1471-2121-11-63.
6. Pumroy RA, Cingolani G. 2015. Diversification of importin-alpha isoforms in cellular trafficking and disease states. Biochem J 466:13–28. https://doi.org/10.1042/BJ20141186.
7. Lott K, Cingolani G. 2011. The importin beta binding domain as a master regulator of nucleocytoplasmic transport. Biochim Biophys Acta 1813:1578–1592. https://doi.org/10.1016/j.bbamcr.2010.10.012.
8. Mason DA, Stage DE, Goldfarb DS. 2009. Evolution of the metazoan-specific importin α gene family. J Mol Evol 68:351–365. https://doi.org/10.1007/s00239-009-9215-8.
9. Tessier TM, Dodge MJ, Prusinkiewicz MA, Mymryk JS. 2019. Viral appropriation: laying claim to host nuclear transport machinery. Cells 8:559. https://doi.org/10.3390/cells8060559.
10. Ghebremedhin B. 2014. Human adenovirus: viral pathogen with increasing importance. Eur J Microbiol Immunol (Bp) 4:26–33. https://doi.org/10.1556/EuJMI.4.2014.1.2.
11. Lion T. 2014. Adenovirus infections in immunocompetent and immunocompromised patients. Clin Microbiol Rev 27:441–462. https://doi.org/10.1128/CMR.00116-13.
12. King CR, Zhang A, Mymryk JS. 2016. The persistent mystery of adenovirus persistence. Trends Microbiol 24:323–324. https://doi.org/10.1016/j.tim.2016.02.007.
13. Lai CY, Lee CJ, Lu CY, Lee PI, Shao PL, Wu ET, Wang CC, Tan BF, Chang HY, Hsia SH, Lin JJ, Chang LY, Huang YC, Huang LM, Taiwan Pediatric Infectious Disease Alliance. 2013. Adenovirus serotype 3 and 7 infection

with acute respiratory failure in children in Taiwan, 2010–2011. PLoS One 8:e53614. https://doi.org/10.1371/journal.pone.0053614.
14. Wo Y, Bin Lu Q, Huang DD, Li XK, Guo CT, Wang HY, Zhang XA, Liu W, Cao WC. 2015. Epidemical features of HAdV-3 and HAdV-7 in pediatric pneumonia in Chongqing, China. Arch Virol 160:633–638. https://doi.org/10.1007/s00705-014-2308-8.
15. Jin Y, Zhang RF, Xie ZP, Yan KL, Gao HC, Song JR, Yuan XH, De Hou Y, Duan ZJ. 2013. Prevalence of adenovirus in children with acute respiratory tract infection in Lanzhou, China. Virol J 10:271. https://doi.org/10.1186/1743-422X-10-271.
16. Lee J, Choi EH, Lee HJ. 2010. Comprehensive serotyping and epidemiology of human adenovirus isolated from the respiratory tract of Korean children over 17 consecutive years (1991–2007). J Med Virol 82:624–631. https://doi.org/10.1002/jmv.21701.
17. Lee WJ, Jung HD, Cheong HM, Kim K. 2015. Molecular epidemiology of a post-influenza pandemic outbreak of acute respiratory infections in Korea caused by human adenovirus type 3. J Med Virol 87:10–17. https://doi.org/10.1002/jmv.23984.
18. Ko J-H, Woo H, Oh HS, Moon SM, Choi JY, Lim JU, Kim D, Byun J, Kwon S-H, Kang D, Heo JY, Peck KR. 2019. Ongoing outbreak of human adenovirus-associated acute respiratory illness in the Republic of Korea military, 2013 to 2018. Korean J Intern Med https://doi.org/10.3904/kjim.2019.092.
19. Lafolie J, Mirand A, Salmona M, Lautrette A, Archimbaud C, Brebion A, Regagnon C, Chambon M, Mercier-Delarue S, Le Goff J, Henquell C. 2016. Severe pneumonia associated with adenovirus type 55 infection, France, 2014. Emerg Infect Dis 22:2012–2014. https://doi.org/10.3201/eid2211.160728.
20. Walsh MP, Seto J, Jones MS, Chodosh J, Xu W, Seto D. 2010. Computational analysis identifies human adenovirus type 55 as a re-emergent acute respiratory disease pathogen. J Clin Microbiol 48:991–993. https://doi.org/10.1128/JCM.01694-09.
21. Salama M, Amitai Z, Amir N, Gottesman-Yekutieli T, Sherbany H, Drori Y, Mendelson E, Carmeli Y, Mandelboim M. 2016. Outbreak of adenovirus type 55 infection in Israel. J Clin Virol 78:31–35. https://doi.org/10.1016/j.jcv.2016.03.002.
22. Khanal S, Ghimire P, Dhamoon AS. 2018. The repertoire of adenovirus in human disease: the innocuous to the deadly. Biomedicines 6:30. https://doi.org/10.3390/biomedicines6010030.
23. Alvarez-Cardona JJ, Whited LK, Chemaly RF. 2020. Brincidofovir: understanding its unique profile and potential role against adenovirus and other viral infections. Future Microbiol 15:389–400. https://doi.org/10.2217/fmb-2019-0288.
24. Berk A. 2013. Adenoviridae, p 1704–1731. *In* Knipe DM, Howley PM (ed), Fields virology. Lippincott Williams and Wilkins, Philadelphia, PA.
25. Pied N, Wodrich H. 2019. Imaging the adenovirus infection cycle. FEBS Lett 593:3419–3448. https://doi.org/10.1002/1873-3468.13690.
26. Babalola OE. 2011. Ocular onchocerciasis: current management and future prospects. Clin Ophthalmol 5:1479–1491. https://doi.org/10.2147/OPTH.S8372.
27. Victoria J, Trujillo R. 2001. Topical ivermectin: a new successful treatment for scabies. Pediatr Dermatol 18:63–65. https://doi.org/10.1046/j.1525-1470.2001.018001063.x.
28. Strycharz JP, Yoon KS, Clark JM. 2008. A new ivermectin formulation topically kills permethrin-resistant human head lice (Anoplura: Pediculidae). J Med Entomol 45:75–81. https://doi.org/10.1093/jmedent/45.1.75.
29. Laing R, Gillan V, Devaney E. 2017. Ivermectin: old drug, new tricks? Trends Parasitol 33:463–472. https://doi.org/10.1016/j.pt.2017.02.004.
30. Romani L, Whitfeld MJ, Koroivueta J, Kama M, Wand H, Tikoduadua L, Tuicakau M, Koroi A, Andrews R, Kaldor JM, Steer AC. 2015. Mass drug administration for scabies control in a population with endemic disease. N Engl J Med 373:2305–2313. https://doi.org/10.1056/NEJMoa1500987.
31. Wagstaff KM, Rawlinson SM, Hearps AC, Jans DA. 2011. An AlphaScreen-based assay for high-throughput screening for specific inhibitors of nuclear import. J Biomol Screen 16:192–200. https://doi.org/10.1177/1087057110390360.
32. Tay MYF, Fraser JE, Chan WKK, Moreland NJ, Rathore AP, Wang C, Vasudevan SG, Jans DA. 2013. Nuclear localization of dengue virus (DENV) 1-4 non-structural protein 5; protection against all 4 DENV serotypes by the inhibitor ivermectin. Antiviral Res 99:301–306. https://doi.org/10.1016/j.antiviral.2013.06.002.
33. Wagstaff KM, Sivakumaran H, Heaton SM, Harrich D, Jans DA. 2012. Ivermectin is a specific inhibitor of importin alpha/beta-mediated nuclear import able to inhibit replication of HIV-1 and dengue virus. Biochem J 443:851–856. https://doi.org/10.1042/BJ20120150.
34. Atkinson SC, Audsley MD, Lieu KG, Marsh GA, Thomas DR, Heaton SM, Paxman JJ, Wagstaff KM, Buckle AM, Moseley GW, Jans DA, Borg NA. 2018. Recognition by host nuclear transport proteins drives disorder-to-order transition in Hendra virus V. Sci Rep 8:358. https://doi.org/10.1038/s41598-017-18742-8.
35. Bennett SM, Zhao L, Bosard C, Imperiale MJ. 2015. Role of a nuclear localization signal on the minor capsid proteins VP2 and VP3 in BKPyV nuclear entry. Virology 474:110–116. https://doi.org/10.1016/j.virol.2014.10.013.
36. Charman M, Herrmann C, Weitzman MD. 2019. Viral and cellular interactions during adenovirus DNA replication. FEBS Lett 593:3531–3550. https://doi.org/10.1002/1873-3468.13695.
37. Fraser JE, Rawlinson SM, Wang C, Jans DA, Wagstaff KM. 2014. Investigating dengue virus nonstructural protein 5 (NS5) nuclear import. Methods Mol Biol 1138:301–328. https://doi.org/10.1007/978-1-4939-0348-1_19.
38. Kalderon D, Roberts BL, Richardson WD, Smith AE. 1984. A short amino acid sequence able to specify nuclear location. Cell 39:499–509. https://doi.org/10.1016/0092-8674(84)90457-4.
39. King CR, Zhang A, Tessier TM, Gameiro SF, Mymryk JS. 2018. Hacking the cell: network intrusion and exploitation by adenovirus E1A. mBio 9:e00390-18. https://doi.org/10.1128/mBio.00390-18.
40. Cohen MJ, King CR, Dikeakos JD, Mymryk JS. 2014. Functional analysis of the C-terminal region of human adenovirus E1A reveals a misidentified nuclear localization signal. Virology 468–470:238–243. https://doi.org/10.1016/j.virol.2014.08.014.
41. Lyons RH, Ferguson BQ, Rosenberg M. 1987. Pentapeptide nuclear localization signal in adenovirus E1a. Mol Cell Biol 7:2451–2456. https://doi.org/10.1128/mcb.7.7.2451.
42. Kohler M, Gorlich D, Hartmann E, Franke J. 2001. Adenoviral E1A protein nuclear import is preferentially mediated by importin alpha3 in vitro. Virology 289:186–191. https://doi.org/10.1006/viro.2001.1151.
43. van Breukelen B, Brenkman AB, Holthuizen PE, van der Vliet PC. 2003. Adenovirus type 5 DNA binding protein stimulates binding of DNA polymerase to the replication origin. J Virol 77:915–922. https://doi.org/10.1128/jvi.77.2.915-922.2003.
44. Hidalgo P, Gonzalez RA. 2019. Formation of adenovirus DNA replication compartments. FEBS Lett 593:3518–3530. https://doi.org/10.1002/1873-3468.13672.
45. Morin N, Delsert C, Klessig DF. 1989. Nuclear localization of the adenovirus DNA-binding protein: requirement for two signals and complementation during viral infection. Mol Cell Biol 9:4372–4380. https://doi.org/10.1128/mcb.9.10.4372.
46. Bekerman E, Einav S. 2015. Combating emerging viral threats. Science 348:282–283. https://doi.org/10.1126/science.aaa3778.
47. De Clercq E, Li G. 2016. Approved antiviral drugs over the past 50 years. Clin Microbiol Rev 29:695–747. https://doi.org/10.1128/CMR.00102-15.
48. De Wit E, Van Doremalen N, Falzarano D, Munster VJ. 2016. SARS and MERS: recent insights into emerging coronaviruses. Nat Rev Microbiol 14:523–534. https://doi.org/10.1038/nrmicro.2016.81.
49. Zhou P, Lou Yang X, Wang XG, Hu B, Zhang L, Zhang W, Si HR, Zhu Y, Li B, Huang CL, Chen HD, Chen J, Luo Y, Guo H, Di Jiang R, Liu MQ, Chen Y, Shen XR, Wang X, Zheng XS, Zhao K, Chen QJ, Deng F, Liu LL, Yan B, Zhan FX, Wang YY, Xiao GF, Shi ZL. 2020. A pneumonia outbreak associated with a new coronavirus of probable bat origin. Nature 579:270–273. https://doi.org/10.1038/s41586-020-2012-7.
50. Lee S-Y, Yen H-L. 2012. Targeting the host or the virus: current and novel concepts for antiviral approaches against influenza virus infection. Antiviral Res 96:391–404. https://doi.org/10.1016/j.antiviral.2012.09.013.
51. Warfield KL, Schaaf KR, DeWald LE, Spurgers KB, Wang W, Stavale E, Mendenhall M, Shilts MH, Stockwell TB, Barnard DL, Ramstedt U, Das SR. 2019. Lack of selective resistance of influenza A virus in presence of host-targeted antiviral, UV-4B. Sci Rep 9:7484. https://doi.org/10.1038/s41598-019-43030-y.
52. Baillie JK. 2014. Translational genomics. Targeting the host immune response to fight infection. Science 344:807–808. https://doi.org/10.1126/science.1255074.
53. Brelot A, Chakrabarti LA. 2018. CCR5 revisited: how mechanisms of HIV entry govern AIDS pathogenesis. J Mol Biol 430:2557–2589. https://doi.org/10.1016/j.jmb.2018.06.027.
54. Kosyna FK, Depping R. 2018. Controlling the gatekeeper: therapeutic

targeting of nuclear transport. Cells 7:221. https://doi.org/10.3390/cells7110221.
55. Yang S, Atkinson S, Fraser J, Wang C, Maher B, Roman N, Forwood J, Wagstaff K, Borg N, Jans D. 2019. Novel flavivirus antiviral that targets the host nuclear transport importin α/β1 heterodimer. Cells 8:281. https://doi.org/10.3390/cells8030281.
56. Jans DA, Martin AJ, Wagstaff KM. 2019. Inhibitors of nuclear transport. Curr Opin Cell Biol 58:50–60. https://doi.org/10.1016/j.ceb.2019.01.001.
57. Varghese FS, Kaukinen P, Glasker S, Bespalov M, Hanski L, Wennerberg K, Kummerer BM, Ahola T. 2016. Discovery of berberine, abamectin and ivermectin as antivirals against chikungunya and other alphaviruses. Antiviral Res 126:117–124. https://doi.org/10.1016/j.antiviral.2015.12.012.
58. Thomas DR, Lundberg L, Pinkham C, Shechter S, DeBono A, Baell J, Wagstaff KM, Hick CA, Kehn-Hall K, Jans DA. 2018. Identification of novel antivirals inhibiting recognition of Venezuelan equine encephalitis virus capsid protein by the importin alpha/beta1 heterodimer through high-throughput screening. Antiviral Res 151:8–19. https://doi.org/10.1016/j.antiviral.2018.01.007.
59. Lv C, Liu W, Wang B, Dang R, Qiu L, Ren J, Yan C, Yang Z, Wang X. 2018. Ivermectin inhibits DNA polymerase UL42 of pseudorabies virus entrance into the nucleus and proliferation of the virus in vitro and vivo. Antiviral Res 159:55–62. https://doi.org/10.1016/j.antiviral.2018.09.010.
60. Jans DA, Martin AJ. 2018. Nucleocytoplasmic trafficking of dengue nonstructural protein 5 as a target for antivirals. Adv Exp Med Biol 1062:199–213. https://doi.org/10.1007/978-981-10-8727-1_15.
61. Yang SNY, Atkinson SC, Wang C, Lee A, Bogoyevitch MA, Borg NA, Jans DA. 2020. The broad spectrum antiviral ivermectin targets the host nuclear transport importin alpha/beta1 heterodimer. Antiviral Res 177:104760. https://doi.org/10.1016/j.antiviral.2020.104760.
62. Caly L, Druce JD, Catton MG, Jans DA, Wagstaff KM. 2020. The FDA-approved drug ivermectin inhibits the replication of SARS-CoV-2 in vitro. Antiviral Res 178:104787. https://doi.org/10.1016/j.antiviral.2020.104787.
63. King CR, Gameiro SF, Tessier TM, Zhang A, Mymryk JS. 2018. Mimicry of cellular A kinase-anchoring proteins is a conserved and critical function of E1A across various human adenovirus species. J Virol 92:e01902-17. https://doi.org/10.1128/JVI.01902-17.
64. Marshall KS, Cohen MJ, Fonseca GJ, Todorovic B, King CR, Yousef AF, Zhang Z, Mymryk JS. 2014. Identification and characterization of multiple conserved nuclear localization signals within adenovirus E1A. Virology 454–455:206–214. https://doi.org/10.1016/j.virol.2014.02.020.
65. Hearing P, Shenk T. 1983. The adenovirus type 5 E1A transcriptional control region contains a duplicated enhancer element. Cell 33:695–703. https://doi.org/10.1016/0092-8674(83)90012-0.
66. Dodding MP, Way M. 2011. Coupling viruses to dynein and kinesin-1. EMBO J 30:3527–3539. https://doi.org/10.1038/emboj.2011.283.
67. Bremner KH, Scherer J, Yi J, Vershinin M, Gross SP, Vallee RB. 2009. Adenovirus transport via direct interaction of cytoplasmic dynein with the viral capsid hexon subunit. Cell Host Microbe 6:523–535. https://doi.org/10.1016/j.chom.2009.11.006.
68. Dehghan S, Seto J, Liu EB, Walsh MP, Dyer DW, Chodosh J, Seto D. 2013. Computational analysis of four human adenovirus type 4 genomes reveals molecular evolution through two interspecies recombination events. Virology 443:197–207. https://doi.org/10.1016/j.virol.2013.05.014.
69. Harreman MT, Cohen PE, Hodel MR, Truscott GJ, Corbett AH, Hodel AE. 2003. Characterization of the auto-inhibitory sequence within the N-terminal domain of importin α. J Biol Chem 278:21361–21369. https://doi.org/10.1074/jbc.M301114200.
70. Montell C, Fisher EF, Caruthers MH, Berk AJ. 1982. Resolving the functions of overlapping viral genes by site-specific mutagenesis at a mRNA splice site. Nature 295:380–384. https://doi.org/10.1038/295380a0.
71. Winberg G, Shenk T. 1984. Dissection of overlapping functions within the adenovirus type 5 E1A gene. EMBO J 3:1907–1912. https://doi.org/10.1002/j.1460-2075.1984.tb02066.x.
72. Crisostomo L, Soriano AM, Frost JR, Olanubi O, Mendez M, Pelka P. 2017. The influence of E1A C-terminus on adenovirus replicative cycle. Viruses 9:387. https://doi.org/10.3390/v9120387.
73. Howley PM, Livingston DM. 2009. Small DNA tumor viruses: large contributors to biomedical sciences. Virology 384:256–259. https://doi.org/10.1016/j.virol.2008.12.006.
74. Tao M, Kruhlak M, Xia S, Androphy E, Zheng Z-M. 2003. Signals that dictate nuclear localization of human papillomavirus type 16 oncoprotein E6 in living cells. J Virol 77:13232–13247. https://doi.org/10.1128/jvi.77.24.13232-13247.2003.
75. Jones N, Shenk T. 1979. Isolation of adenovirus type 5 host range deletion mutants defective for transformation of rat embryo cells. Cell 17:683–689. https://doi.org/10.1016/0092-8674(79)90275-7.